Supplementary Information

S1   Algorithm for Cross-Validated scPCA

Algorithm 1: Cross-validated scPCA

Result: Produces a sparse low-dimensional representation of the target data, $\mathbf{X}_{n \times p}$, by contrasting the variation of $\mathbf{X}_{n \times p}$ and some background data, $\mathbf{Y}_{m \times p}$, while applying an ℓ_1 penalty to the loadings generated by cPCA.

Input :

  target dataset: $\mathbf{X}$

  background dataset: $\mathbf{Y}$

  binary variable indicating whether to column-scale the data: `scale`

  vector of possible contrastive parameters: $\gamma = (\gamma_1, \ldots, \gamma_s)$

  vector of possible ℓ_1 penalty parameters: $\lambda_1 = (\lambda_{1,1}, \ldots, \lambda_{1,d})$

  number of sparse contrastive principal components to compute: k

  clustering method: `cluster_meth`

  number of clusters: `ncluster`

  number of cross-validation folds: V

For $\mathbf{X}_{n \times p}$, randomly partition the index set $\{1, \ldots, n\}$ into V validation sets, $\mathcal{V}_1^x, \ldots, \mathcal{V}_V^x$, of (approximately) the same size (i.e., $\bigcup_{v=1}^V \mathcal{V}_v^x = \{1, \ldots, n\}$; $\mathcal{V}_v^x \cap \mathcal{V}_{v'}^x = \emptyset, \quad \forall v, v' \in \{1, \ldots, V\}$). Denote the corresponding training sets by $\mathcal{T}_v^x = \{1, \ldots, n\} \setminus \mathcal{V}_v^x$. For $\mathbf{Y}_{m \times p}$, randomly partition the index set $\{1, \ldots, m\}$ into V validation sets, $\mathcal{V}_1^y, \ldots, \mathcal{V}_V^y$, of (approximately) the same size (i.e., $\bigcup_{v=1}^V \mathcal{V}_v^y = \{1, \ldots, m\}$; $\mathcal{V}_v^y \cap \mathcal{V}_{v'}^y = \emptyset, \quad \forall v, v' \in \{1, \ldots, V\}$). Denote the corresponding training sets by $\mathcal{T}_v^y = \{1, \ldots, m\} \setminus \mathcal{V}_v^y$. Denote by $\mathbf{X}_{\mathcal{T}_v^x}$ the $(n - |\mathcal{T}_v^x|) \times p$ submatrix of $\mathbf{X}$ for training set $\mathcal{T}_v^x$ and by $\mathbf{Y}_{\mathcal{T}_v^y}$ the $(m - |\mathcal{T}_v^y|) \times p$ submatrix of $\mathbf{Y}$ for training set $\mathcal{T}_v^y$. Define similarly $\mathbf{X}_{\mathcal{V}_v^x}$ and $\mathbf{Y}_{\mathcal{V}_v^y}$ for the validation sets. Note that $\mathbf{Y}_{\mathcal{V}_v^y}$ is defined explicitly solely to avoid ambiguity; it plays no role in subsequent developments.

for *each v in* $\{1, \ldots, V\}$ **do**

  Center (and `scale` if so desired) the columns of $\{\mathbf{X}_{\mathcal{T}_v^x}, \mathbf{Y}_{\mathcal{T}_v^y}\}$ and $\{\mathbf{X}_{\mathcal{V}_v^x}, \mathbf{Y}_{\mathcal{V}_v^y}\}$

  Compute the empirical covariance matrices: $\mathbf{C}_{\mathbf{X}_{p \times p}} := \frac{1}{|\mathcal{T}_v^x|} \mathbf{X}_{\mathcal{T}_v^x}^\top \mathbf{X}_{\mathcal{T}_v^x}, \; \mathbf{C}_{\mathbf{Y}_{p \times p}} := \frac{1}{|\mathcal{T}_v^y|} \mathbf{Y}_{\mathcal{T}_v^y}^\top \mathbf{Y}_{\mathcal{T}_v^y}$

  for *each $\gamma_i \in \gamma$* **do**

   for *each $\lambda_{1,j} \in \lambda_1$* **do**

    Compute the contrastive covariance matrix $\mathbf{C}_{\gamma_i} = \mathbf{C}_{\mathbf{X}} - \gamma_i \mathbf{C}_{\mathbf{Y}}$

    Compute the positive-semidefinite approximation of $\mathbf{C}_{\gamma_i}$, $\widetilde{\mathbf{C}}_{\gamma_i}$

    Apply SPCA to $\widetilde{\mathbf{C}}_{\gamma_i}$ for k components with ℓ_1 penalty $\lambda_{1,j}$

    Generate a low-dimensional representation of the target validation set by projecting $\mathbf{X}_{\mathcal{V}_v^x}$ on the sparse loadings of SPCA

    Normalize the low-dimensional representation produced to be on the unit hypercube

    Cluster the normalized low-dimensional representation using `cluster_meth` with `ncluster`

    Compute and record the clustering strength criterion associated with $(\gamma_i, \lambda_{1,j})$

Identify the combination of hyperparameters maximizing the cross-validated mean (across all folds $\{1, \ldots, V\}$) of the clustering strength criterion: $\gamma^\star, \lambda_1^\star$

Output: The low-dimensional representation of the target data given by $(\gamma^\star, \lambda_1^\star)$, a $n \times k$ matrix; the $p \times k$ matrix of loadings given by $(\gamma^\star, \lambda_1^\star)$; contrastive parameter $\gamma^\star$; ℓ_1 penalty parameter $\lambda_1^\star$

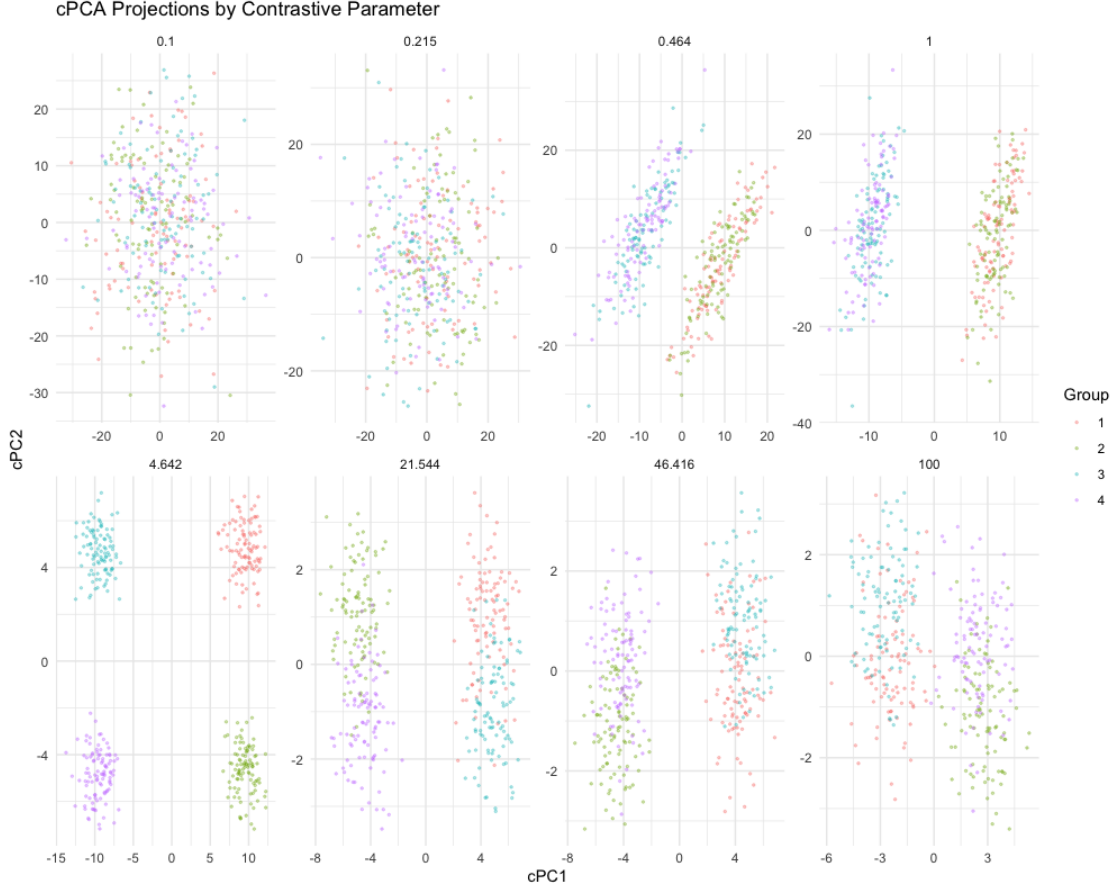## S2   Contrastive Parameter Intuition

Figure S1:   *Effect of contrastive parameter for cPCA.* cPCA as implemented by Abid et al. was applied to a simulated dataset of $n = 400$ observations, split across 4 groups, with $p = 30$ variables. The first 10 variables are distributed as $N(0, 10)$ for all observations. Variables 11 through 20 are distributed as $N(0, 1)$ for Groups 1 an 2, and as $N(3, 1)$ for Groups 3 and 4. Variables 21 through 30 are distributed as $N(-3, 1)$ for Groups 1 and 3, and as $N(0, 1)$ for Groups 2 and 4. cPCA also takes as input a background dataset of $m = 400$ observations, with $p = 30$ variables, where the first 10 variables are distributed as $N(0, 10)$, the following 10 as $N(0, 3)$, and the remaining 10 as $N(0, 1)$. The results of cPCA are then presented for eight increasing values of the contrastive parameter γ, selected using the technique described by Abid et al. For the smaller values of the contrastive parameter, the noise contained in the first 10 variables of the target data dominates the signal contained in variables 11 through 30. As the contrastive parameter increases, the signal in the target data set is unmasked. However, once the contrastive parameter value becomes larger than ≈ 20, the distinction between groups becomes increasingly poor; the variation contained in the background data begins to dominate the variation contained in the target data. A virtually identical dataset is presented in the supplementary material of Abid et al.

S3   Simulated Data

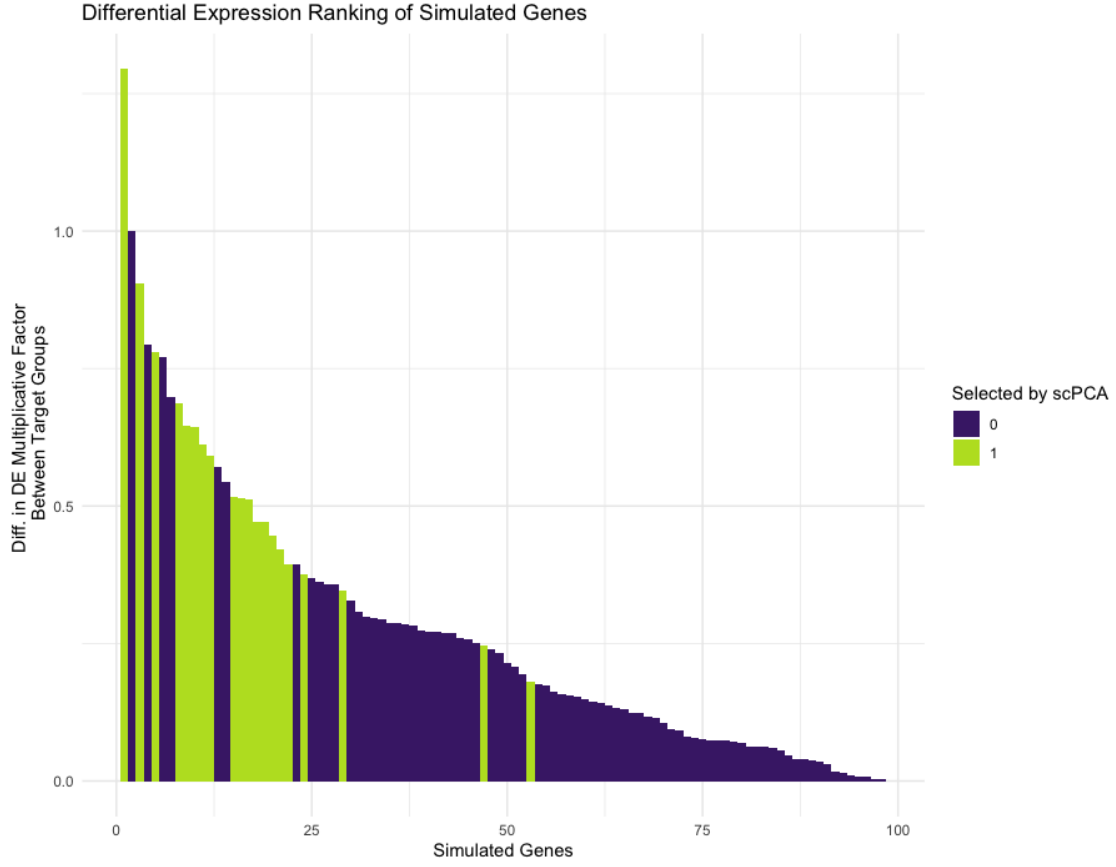See Section 3.1 for information on the simulation model and dataset.

Figure S2: *Simulated scRNA-seq data: Differential expression.* The 98 differentially expressed genes in the simulated target dataset are ranked in decreasing order of their absolute level of differential expression between groups. In the *Splatter* framework, genes are differentially expressed between groups by way of a group-specific multiplicative factor. Thus, the level of differential expression of any gene between two groups may be computed as the absolute value of the difference between each groups multiplicative factor. We find that all 20 of the genes with non-zero entries in scPCA's first loading vector, highlighted in green, are among the most differentially expressed.
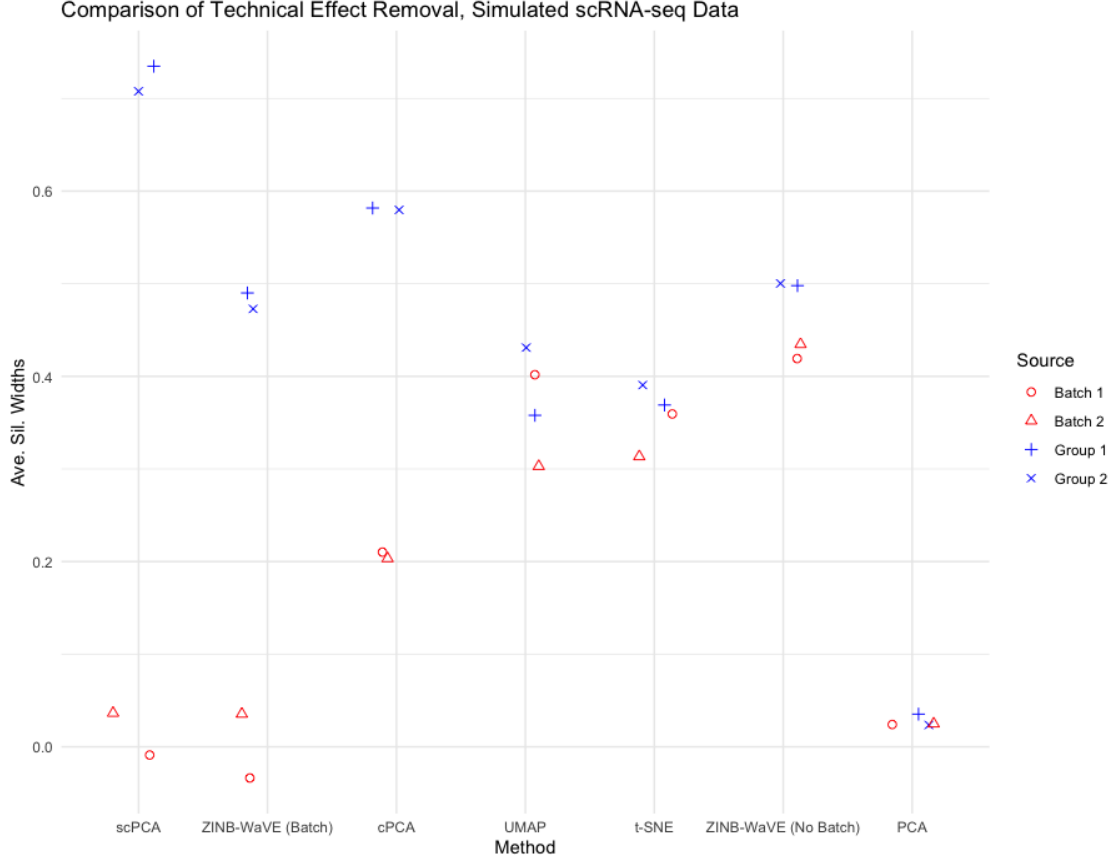
Figure S3: *Simulated scRNA-seq data: Average silhouette width comparison.* scPCA produces the densest biological clusters with the least amount of technical noise. The ZINB-WaVE method, when taking into account the batch effect, has a similar performance to scPCA with respect to the removal of unwanted effects, though the biological clusters it produces have lower average silhouette widths. Though cPCA produces denser biological clusters than ZINB-WaVE, it fails to completely remove the batch effect. The remaining methods are unable to disentangle the biological and technical effects.

S4   Dengue Microarray Data

See Section 3.2 for information on the data.

Table S1: *Dengue microarray data: Genes with non-zero weights in the first scPCA loadings vector.*

	Gene Symbol	Gene Name	Weight
1	PRSS33	protease, serine, 33	-0.0059
2	PDZK1IP1	PDZK1 interacting protein 1	-0.0347
3	SDC1	syndecan 1	0.2507
4	CAV1	caveolin 1, caveolae protein, 22kDa	0.0889
5	GGH	gamma-glutamyl hydrolase (conjugase, folylpolygam-maglutamyl hydrolase)	0.2318
6	PI3	peptidase inhibitor 3, skin-derived	-0.0209
7	BUB1B	budding uninhibited by benzimidazoles 1 homolog beta (yeast)	0.1242
8	ZWINT	ZW10 interactor	0.3984
9	TUBB2A	tubulin, beta 2A	-0.0004

4

Table S1: *Dengue microarray data: Genes with non-zero weights in the first scPCA loadings vector.*

	Gene Symbol	Gene Name	Weight
10	PTGS2	prostaglandin-endoperoxide synthase 2 (prostaglandin G/H synthase and cyclooxygenase)	-0.0627
11	TTK	TTK protein kinase	0.0201
12	ORM1 /// ORM2	orosomucoid 1 /// orosomucoid 2	-0.0055
13	CD38	CD38 molecule	0.0399
14	CHI3L1	chitinase 3-like 1 (cartilage glycoprotein-39)	-0.0384
15	HLA-DQB1	major histocompatibility complex, class II, DQ beta 1	0.0720
16	BUB1	budding uninhibited by benzimidazoles 1 homolog (yeast)	0.0853
17	CDK1	cyclin-dependent kinase 1	0.2650
18	IGH@ /// IGHA1 /// IGHA2 /// IGHD /// IGHG1 /// IGHG3 /// IGHG4 /// IGHM /// IGHV4-31 /// LOC100290146 /// LOC100290528	immunoglobulin heavy locus /// immunoglobulin heavy constant alpha 1 /// immunoglobulin heavy constant alpha 2 (A2m marker) /// immunoglobulin heavy constant delta /// immunoglobulin heavy constant gamma 1 (G1m marker) /// immunoglobulin heavy constant gamma 3 (G3m marker) /// immunoglobulin heavy constant gamma 4 (G4m marker) /// immunoglobulin heavy constant mu /// immunoglobulin heavy variable 4-31 /// hypothetical protein LOC100290146 /// similar to pre-B lymphocyte gene 2	0.0180
19	IGH@ /// IGHA1 /// IGHA2 /// IGHD /// IGHG1 /// IGHG3 /// IGHG4 /// IGHM /// IGHV3-23 /// LOC100126583 /// LOC100290146 /// LOC652128	immunoglobulin heavy locus /// immunoglobulin heavy constant alpha 1 /// immunoglobulin heavy constant alpha 2 (A2m marker) /// immunoglobulin heavy constant delta /// immunoglobulin heavy constant gamma 1 (G1m marker) /// immunoglobulin heavy constant gamma 3 (G3m marker) /// immunoglobulin heavy constant gamma 4 (G4m marker) /// immunoglobulin heavy constant mu /// immunoglobulin heavy variable 3-23 /// hypothetical LOC100126583 /// hypothetical protein LOC100290146 /// similar to Ig heavy chain V-II region ARH-77 precursor	0.1867
20	NOV	nephroblastoma overexpressed gene	-0.0619
21	SELENBP1	selenium binding protein 1	-0.1315
22	IGHA1 /// IGHG1 /// IGHM /// LOC100290293	immunoglobulin heavy constant alpha 1 /// immunoglobulin heavy constant gamma 1 (G1m marker) /// immunoglobulin heavy constant mu /// similar to hCG2042717	0.0162
23	CEP55	centrosomal protein 55kDa	0.2863
24	PBK	PDZ binding kinase	0.1358
25	SHCBP1	SHC SH2-domain binding protein 1	0.2901
26	MGC29506	plasma cell-induced ER protein 1	0.4012
27	CNTNAP3	contactin associated protein-like 3	-0.0494
28	JAZF1	JAZF zinc finger 1	-0.0441
29	KIAA1324	KIAA1324	-0.0962
30	CDCA2	cell division cycle associated 2	0.3858
31	KLHL14	kelch-like 14 (Drosophila)	0.0801
32	CYAT1	cyclosporin A transporter 1	0.1657

Table S1: *Dengue microarray data: Genes with non-zero weights in the first scPCA loadings vector.*

	Gene Symbol	Gene Name	Weight
33	HLA-DRB1 /// HLA-DRB3 /// HLA-DRB4 /// HLA-DRB5 /// LOC100294036	major histocompatibility complex, class II, DR beta 1 /// major histocompatibility complex, class II, DR beta 3 /// major histocompatibility complex, class II, DR beta 4 /// major histocompatibility complex, class II, DR beta 5 /// similar to HLA class II histocompatibility antigen, DRB1-7 beta chain	0.0422
34	FLJ10357	protein SOLO	-0.0966

Table S2: *Dengue microarray data: Genes with non-zero weights in the second scPCA loadings vector.*

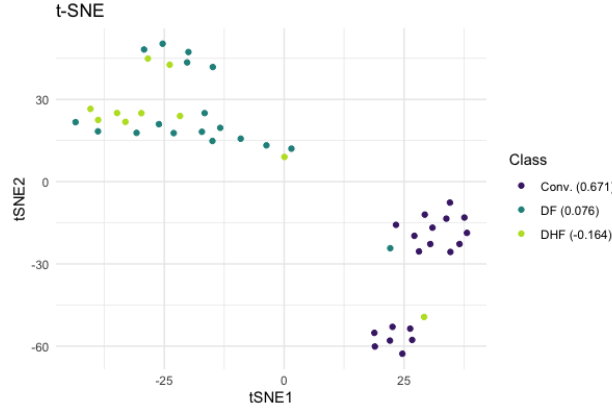|	Gene Symbol	Gene Name	Weight
1	PRSS33	protease, serine, 33	0.1822
2	IFI27	interferon, alpha-inducible protein 27	-0.0147
3	PI3	peptidase inhibitor 3, skin-derived	0.1692
4	SLC2A5	solute carrier family 2 (facilitated glucose/fructose transporter), member 5	0.0701
5	MYOM2	myomesin (M-protein) 2, 165kDa	-0.0278
6	HLA-DRB4	major histocompatibility complex, class II, DR beta 4	-0.0620
7	IGH@ /// IGHA1 /// IGHD /// IGHG1 /// IGHG3 /// IGHG4 /// IGHM /// IGHV3-23 /// IGHV4-31 /// LOC100290146 /// LOC100290528	immunoglobulin heavy locus /// immunoglobulin heavy constant alpha 1 /// immunoglobulin heavy constant delta /// immunoglobulin heavy constant gamma 1 (G1m marker) /// immunoglobulin heavy constant gamma 3 (G3m marker) /// immunoglobulin heavy constant gamma 4 (G4m marker) /// immunoglobulin heavy constant mu /// immunoglobulin heavy variable 3-23 /// immunoglobulin heavy variable 4-31 /// hypothetical protein LOC100290146 /// similar to pre-B lymphocyte gene 2	0.4987
8	IGKV3-20	Immunoglobulin kappa variable 3-20	0.1623
9	RSAD2	radical S-adenosyl methionine domain containing 2	-0.2294
10	USP18	ubiquitin specific peptidase 18	-0.4599
11	SIGLEC1	sialic acid binding Ig-like lectin 1, sialoadhesin	-0.2750
12	KCTD14	potassium channel tetramerisation domain containing 14	-0.3142
13	FAM118A	family with sequence similarity 118, member A	-0.1382
14			0.0269
15	SLC16A14	solute carrier family 16, member 14 (monocarboxylic acid transporter 14)	0.3232
16	ANKRD22	ankyrin repeat domain 22	-0.2800
17	KLC3	kinesin light chain 3	0.1021
18	SIGLEC1	sialic acid binding Ig-like lectin 1, sialoadhesin	-0.0434

Figure S4: *Dengue microarray data: t-SNE.* Similarly to UMAP, t-SNE almost completely separates the convalescent patients from those with some form of dengue. The two main clusters are further split into distinct sub-clusters, perhaps indicating the presence of a batch effect.
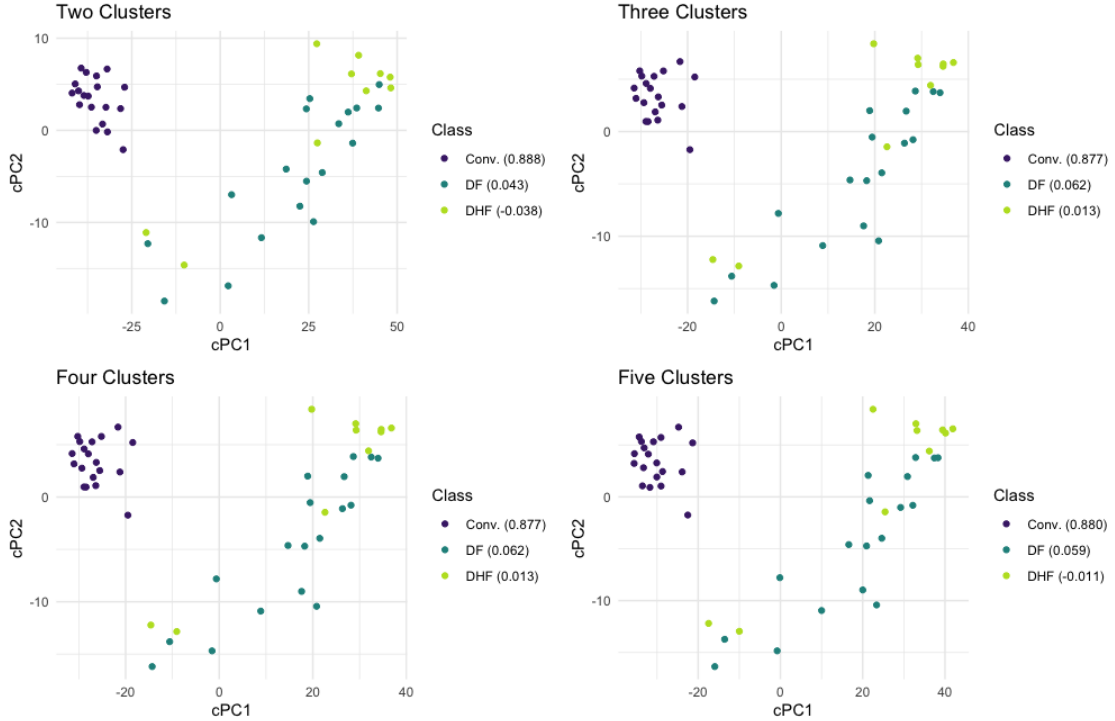

Figure S5: *Dengue microarray data: cPCA.* When varying the *a priori* specified number of clusters for cPCA, all four embeddings are virtually identical, suggesting that optimal contrastive parameters were selected in each case. Thus, cPCA is robust to misspecifications of the number of clusters.
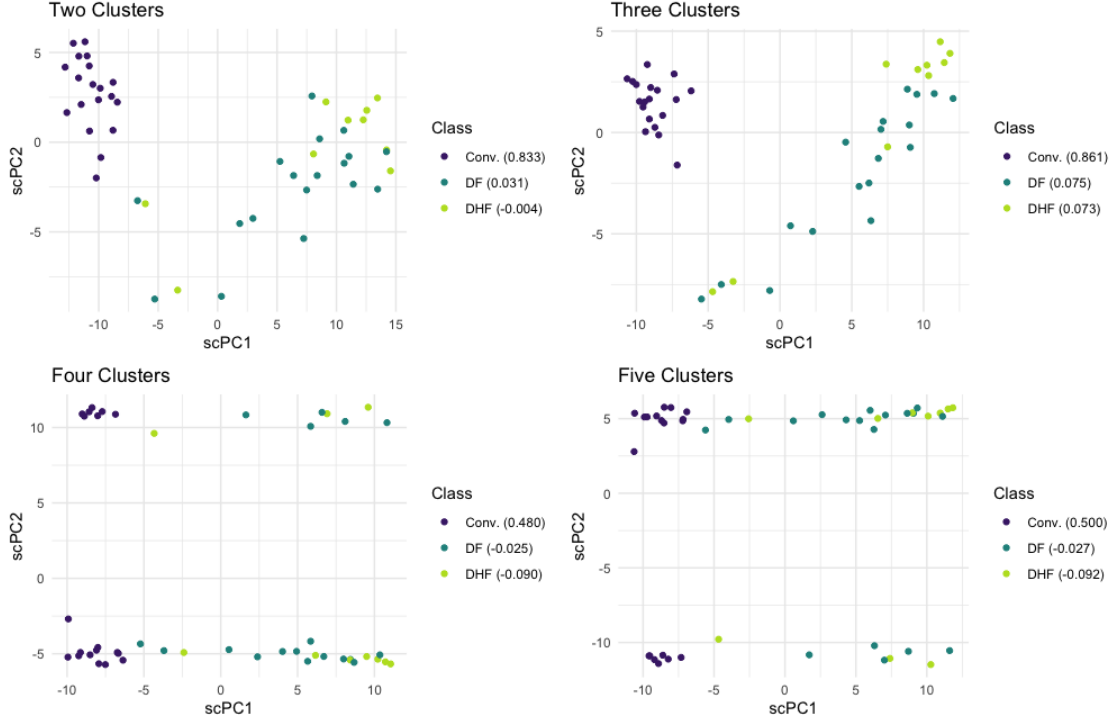
7

Figure S6: *Dengue microarray data: scPCA.* When varying the *a priori* specified number of clusters for scPCA, we find that the two-dimensional embeddings are sensitive to this choice. When scPCA is performed on this data with four and five clusters, the results resemble those produced by PCA.

S5   Leukemia Patient scRNA-seq Data

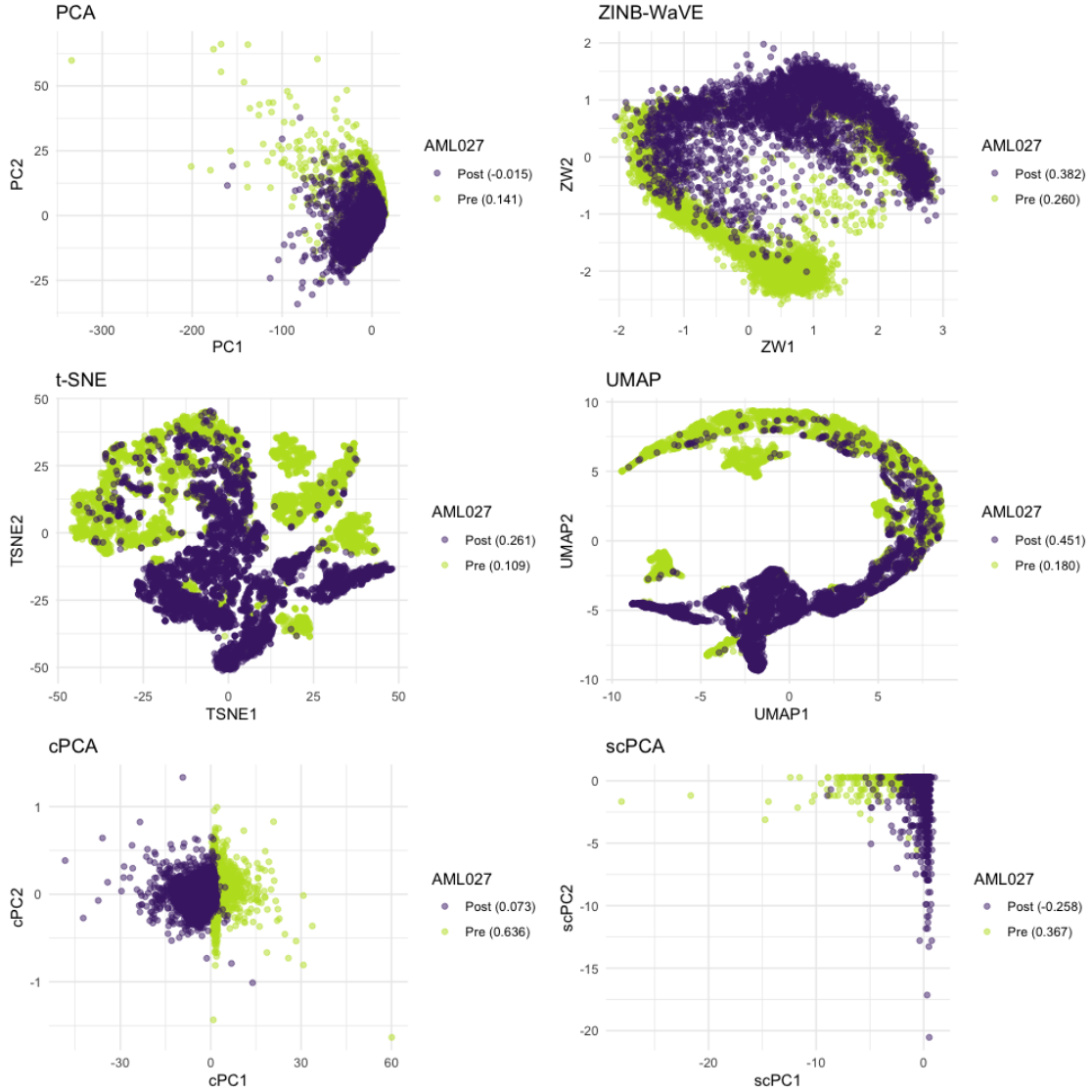See Section 3.3 for information on the data.

Figure S7: *AML Patient 027 scRNA-seq data.* The two-dimensional embeddings of the patient's BMMC cells produced by PCA, ZINB-WaVE, t-SNE, UMAP, cPCA, and scPCA. cPCA and scPCA produce two-dimensional representations that distinguish between the pre- and post-transplant cells of Patient 027. Although cPCA's embedding contains denser clusters, scPCA's clusters are more distinct — though they are oddly shaped. This is the result of sparsity: the scPCA embedding is produced with the count data of only three genes.

S6   Mouse Protein Expression Data

Down Syndrome, the leading genetic cause of intellectual disability [5], is the result of trisomy of all or part of the long arm of chromosome 21 [2]. Recently, researchers have begun exploring the use of pharmacotherapies to mitigate these cognitive deficits using the Ts65Dn mouse model [2, 4]. Though not a perfect model for the study of Down Syndrome, the Ts65Dn displays many relevant neurological phenotypic features, such as deficits in learning and memory [8].

Ahmed et al. [2] analyzed protein expression in the hippocampus and cortex of Ts65Dn and control mice after exposure to context fear conditioning and Memantine treatment. Memantine, a drug often prescribed to Alzheimer's patients, has been demonstrated to improve performance of the Ts65Dn in tasks that reflect cognitive abilities [2]. The corresponding dataset was made available by Higuera et al. [4]. The data consist of normalized expression measures for 77 proteins from subcellular fractions of the cortex assayed from 38 control and 34 Ts65Dn mice. Each protein expression measurement was repeated 15 times (i.e., 15 technical replicates per mouse for each of the 77 proteins), though a small number of replicates contain missing protein expression measurements due to technical artifacts [4]. More details on the experimental design are provided in fig. S8.
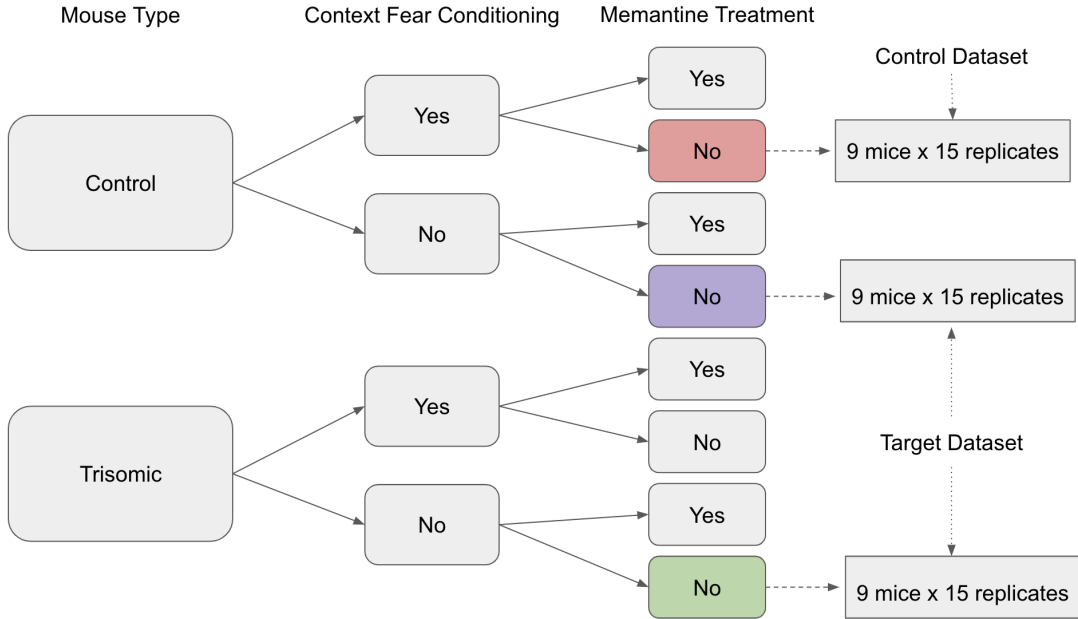

Figure S8:   *Mouse protein expression data: Experimental design.* The control dataset is comprised of protein expression measurements for 15 technical replicates from each of 9 control mice subject to context fear conditioning and given a placebo (red leaf). The target dataset consists of protein expression measurements for 15 technical replicates from each of 9 control mice not subject to context fear condition and given a placebo (purple leaf) and 15 technical replicates from each of 9 trisomic mice not subject to context fear condition and given a placebo (green leaf).

To demonstrate scPCA's capacity to capture biologically meaningful and interpretable variation in protein expression data, the technical replicates of the subset comprising 9 control and 9 Ts65Dn mice not subject to context fear conditioning and given a placebo were designated as the target dataset. The technical replicates of the subset of 9 control mice that were subject to context fear conditioning and given a placebo made up the background dataset, as the variation in their protein expression measurements are believed to be similar to that found in the control mice of the target dataset. The data are identical to those used by Abid et al. [1] to demonstrate cPCA. PCA, t-SNE, UMAP, cPCA, and scPCA were applied to the target dataset (fig. S9A) to identify differences in protein expression between the control and trisomic mice not exposed to the context fear conditioning experiment. In addition to the target dataset, cPCA and scPCA took as input the column-centered background dataset and specified two clusters *a priori*. The embedding produced by t-SNE is substantially worse than other methods because it generates spurious sub-clusters (fig. S10).

PCA proved incapable of distinguishing between the biological groups of interest. UMAP, cPCA, and scPCA successfully split the control and trisomic mice into virtually distinct clusters, though the number of clusters found by UMAP and cPCA in two dimensions did not match, even when varying the *a priori* specified number of clusters in cPCA (fig. S11). Comparing the results of UMAP and scPCA, we find that they produce the same number of clusters, but their representations of the global structure are markedly different, even when varying the number of clusters specified *a priori* in scPCA (fig. S12). The presence of distinct Ts65Dn clusters in UMAP's representation may correspond to technical noise that is diminished in cPCA's and scPCA's embeddings, or may arise from UMAP's inability to dependably capture global structure. We also remark that cPCA and scPCA produce very similar embeddings, up to a rotation; however, the first and second columns of scPCA's loadings matrix contain merely 12 and 16 non-zero entries, respectively (fig. S9B). Also note that the the separation of control and trisomic mice by scPCA only occurs in scPC2: the proteins with non-zero weights in its corresponding loading vector include AKT, APP, SOD1, and GSK3, each of which has been associated with Down Syndrome in human or mouse models [9, 7, 3, 6]. The full list of proteins with non-zero weights in the first two loadings vectors of scPCA are provided in Table S3 and Table S4.

Table S3: *Mouse protein expression data: Proteins with non-zero weights in the first scPCA loadings vector.*

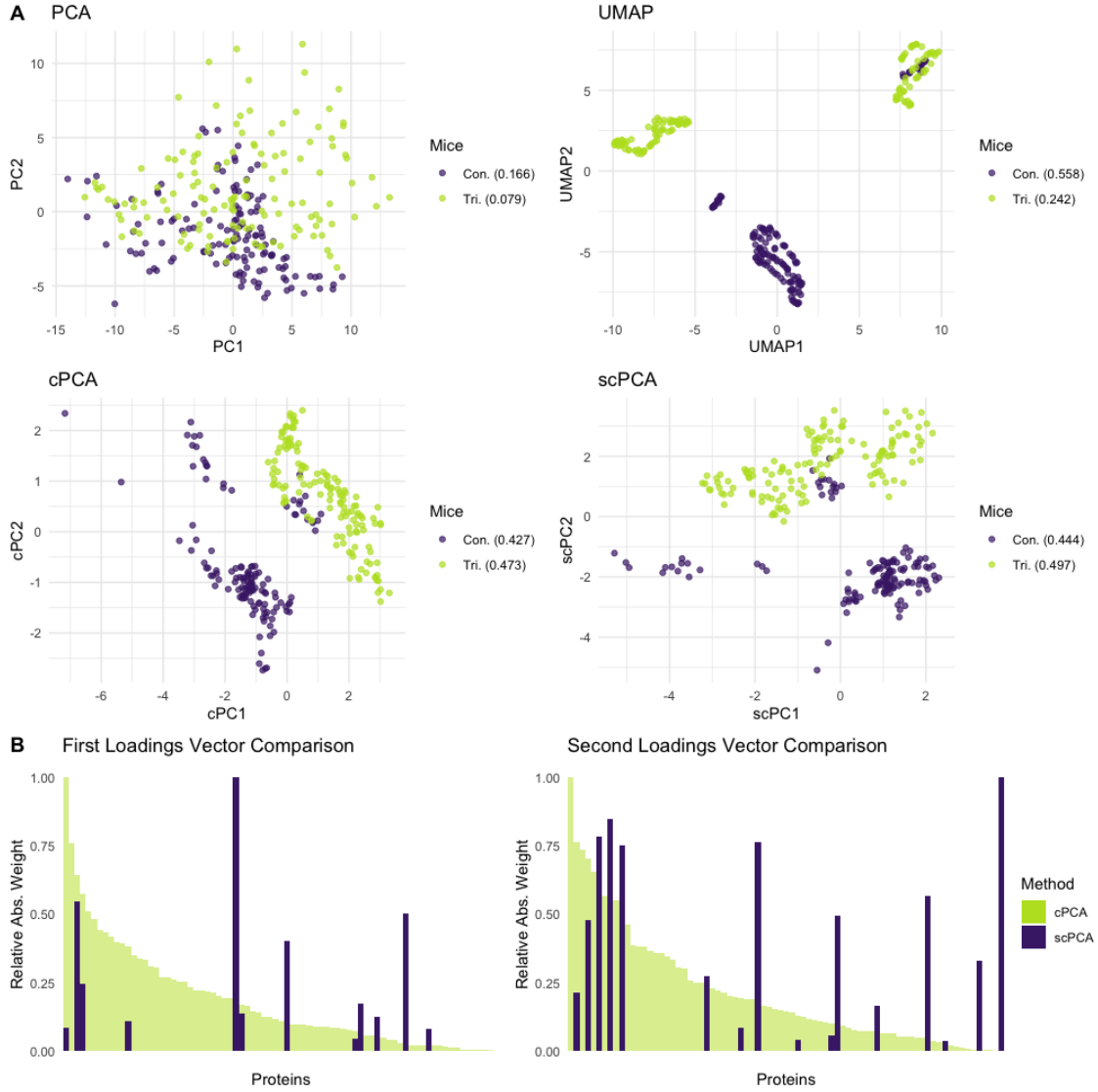|	Protein Symbol	Weight
1	ELK	0.0618
2	BRAF	-0.1001
3	RSK	-0.0927
4	SOD1	0.1800
5	S6	0.1281
6	AcetylH3K9	0.3992
7	RRP1	0.0606
8	Tau	0.7320
9	CASP9	-0.0795
10	PSD95	-0.0329
11	Ubiquitin	-0.3674
12	H3AcK18	0.2958

Figure S9: *Mouse protein expression data.* **A** All methods but PCA were capable of separating the control from the trisomic mice, though it is unclear why UMAP splits the Ts65Dn mice into two distinct groups. scPCA's low-dimensional representation of the protein expression data is markedly similar to that of cPCA, up to a rotation, despite relying on only a fraction of non-zero values in the loadings matrix. On average, scPCA also produces the tightest clusters. Note: a small group of control mice were clustered with the trisomic mice in the UMAP, cPCA, and scPCA representation, potentially comprising a group of mislabeled mice. **B** scPCA's leading vectors of loadings are much sparser than those of cPCA, increasing the interpretability of findings and clarity of the visualization. The differing rotations of cPCA and scPCA, in addition to the drastically different weighting scheme of the proteins in their respective loadings matrices, may indicate that the contrastive step performed by cPCA does not sufficiently dampen spurious sources of variation in the data.
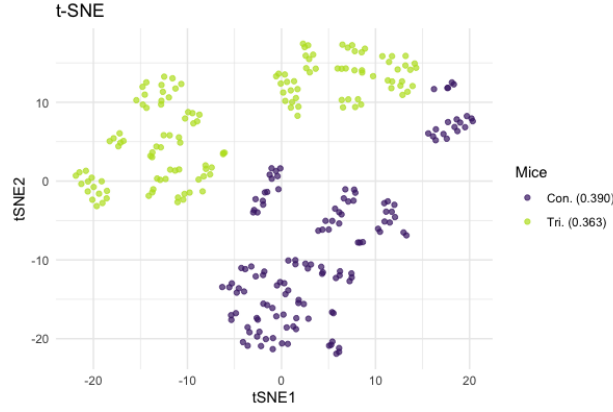
Figure S10: *Mouse protein expression data: t-SNE.* t-SNE produces almost linearly-separable clusters, though these clusters contain many fractured, spurious sub-clusters that do not relate to biological signal.
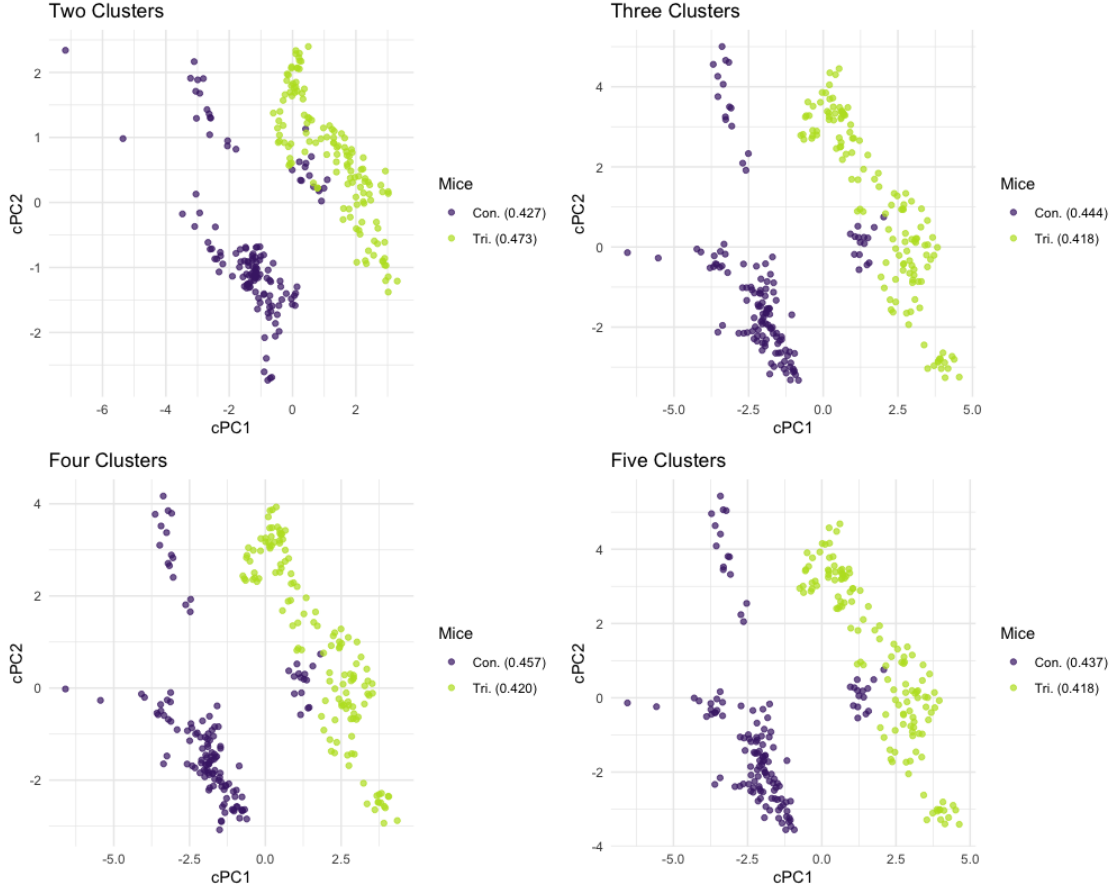

Figure S11: *Mouse protein expression data: cPCA.* When varying the *a priori* specified number of clusters for cPCA, we find that the two-dimensional embedding is once again robust to misspecifications.
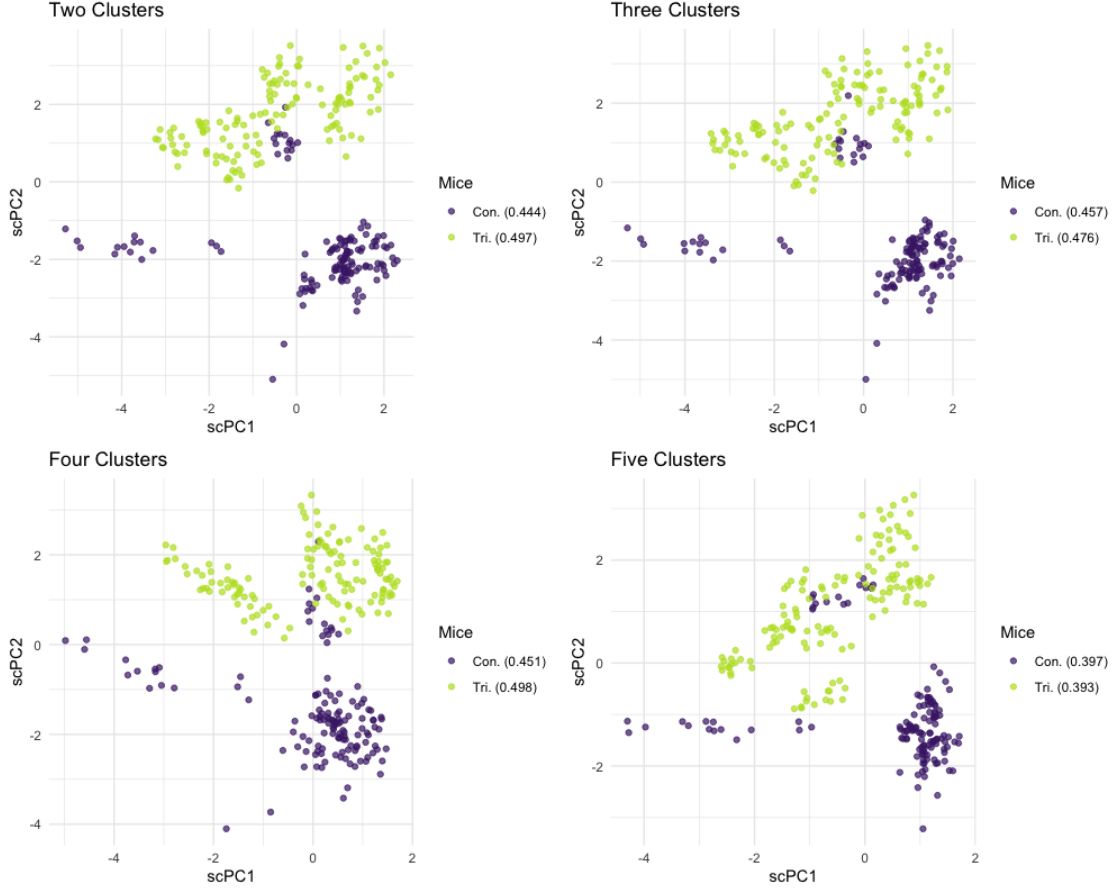
13

Figure S12: *Mouse protein expression data: scPCA.* Unlike with the dengue microarray data, when varying the *a priori* specified number of clusters for scPCA, we find that the two-dimensional embedding is robust to misspecifications. This may indicate that the sensitivity of the method to this tuning parameter is data-dependent.

Table S4: *Mouse protien expression data: Proteins with non-zero weights in the second scPCA loadings vector.*

	Protein Symbol	Weight
1	ELK	-0.2236
2	AKT	-0.0999
3	APP	0.3525
4	SOD1	-0.2323
5	NUMB	0.4690
6	P70S6	0.1554
7	GSK3B	0.3574
8	PKCG	0.3978
9	S6	0.3674
10	RRP1	0.0272
11	GluR4	0.0404
12	IL1B	-0.2664
13	P3525	0.0196
14	PSD95	-0.1289
15	SNCA	-0.0783
16	H3AcK18	0.0169

Supplementary Information References

[1] Abid, A., Zhang, M. J., Bagaria, V. K., and Zou, J. (2018). Exploring patterns enriched in a dataset with contrastive principal component analysis. *Nature Communications*, **9**(1), 2134.

[2] Ahmed, M. M., Dhanasekaran, A. R., Block, A., Tong, S., Costa, A. C. S., Stasko, M., and Gardiner, K. J. (2015). Protein Dynamics Associated with Failed and Rescued Learning in the Ts65Dn Mouse Model of Down Syndrome. *PLOS ONE*, **10**(3), e0119491.

[3] Gulesserian, T., Seidl, R., Hardmeier, R., Cairns, N., and Lubec, G. (2001). Superoxide Dismutase SOD1, Encoded on Chromosome 21, but Not SOD2 Is Overexpressed in Brains of Patients With Down Syndrome. *Journal of Investigative Medicine*, **49**(1), 41–46.

[4] Higuera, C., Gardiner, K. J., and Cios, K. J. (2015). Self-Organizing Feature Maps Identify Proteins Critical to Learning in a Mouse Model of Down Syndrome. *PLOS ONE*, **10**(6), e0129126.

[5] Irving, C., Basu, A., Richmond, S., Burn, J., and Wren, C. (2008). Twenty-year trends in prevalence and survival of Down syndrome. *European Journal of Human Genetics*, **16**(11), 1336–1340.

[6] Isacson, O., Seo, H., Lin, L., Albeck, D., and Granholm, A. C. (2002). Alzheimer's disease and Down's syndrome: Roles of APP, trophic factors and ACh.

[7] Niceta, M., Stellacci, E., Gripp, K. W., Zampino, G., Kousi, M., Anselmi, M., Traversa, A., Ciolfi, A., Stabley, D., Bruselles, A., Caputo, V., Cecchetti, S., Prudente, S., Fiorenza, M. T., Boitani, C., Philip, N., Niyazov, D., Leoni, C., Nakane, T., Keppler-Noreuil, K., Braddock, S. R., Gillessen-Kaesbach, G., Palleschi, A., Campeau, P. M., Lee, B. H., Pouponnot, C., Stella, L., Bocchinfuso, G., Katsanis, N., Sol-Church, K., and Tartaglia, M. (2015). Mutations impairing GSK3-mediated MAF phosphorylation cause cataract, deafness, intellectual disability, seizures, and a down syndrome-like facies. *American Journal of Human Genetics*, **96**(5), 816–825.

[8] Rueda, N., Flórez, J., and Martínez-Cué, C. (2012). Mouse Models of Down Syndrome as a Tool to Unravel the Causes of Mental Disabilities. *Neural Plasticity*, **2012**, 1–26.

[9] Troca-Marín, J. A., Alves-Sampaio, A., and Montesinos, M. L. (2011). An increase in basal bdnf provokes hyperactivation of the akt-mammalian target of rapamycin pathway and deregulation of local dendritic translation in a mouse model of down's syndrome. *Journal of Neuroscience*, **31**(26), 9445–9455.